Dimerization of the Exocyst Protein Sec6p and Its Interaction with the t-SNARE Sec9p†

Mylavarapu V. S. Sivaram, Jennifer A. Saporita, Melonnie L. M. Furgason, Angela J. Boettcher, and Mary Munson*

Department of Biochemistry and Molecular Pharmacology, University of Massachusetts Medical School, Worcester, Massachusetts 01605

Received September 15, 2004; Revised Manuscript Received January 21, 2005

ABSTRACT: Vesicles in eukaryotic cells transport cargo between functionally distinct membrane-bound organelles and the plasma membrane for growth and secretion. Trafficking and fusion of vesicles to specific target sites are highly regulated processes that are not well understood at the molecular level. At the plasma membrane, tethering and fusion of secretory vesicles require the exocyst complex. As a step toward elucidation of the molecular architecture and biochemical function(s) of the exocyst complex, we expressed and purified the exocyst subunit Sec6p and demonstrated that it is a predominantly helical protein. Biophysical characterization of purified Sec6p by gel filtration and analytical ultracentrifugation experiments revealed that Sec6p is a dimer. Limited proteolysis defined an independently folded C-terminal domain (residues 300−805) that equilibrated between a dimer and monomer in solution. Removal of residues 300−410 from this construct yielded a well-folded, monomeric domain. These results demonstrate that residues 300−410 are necessary for dimerization, and the presence of the N-terminal region (1−299) increases dimer stability. Moreover, we found that the dimer of Sec6p binds to the plasma membrane t-SNARE Sec9p and inhibits the interaction between Sec9p and its partner t-SNARE Sso1p. This direct interaction between the exocyst complex and the t-SNARE implicates the exocyst in SNARE complex regulation.

In eukaryotic cells, vesicle-mediated transport is required to transfer membrane and luminal contents between organelles and export materials to the cell surface. Specific trafficking of vesicles to their target membrane is necessary for maintaining the appropriate organization of membrane compartments in the cell, as well as ensuring cell survival and growth. Regulation of membrane targeting and fusion has been attributed to a number of essential cellular factors, including the soluble NSF attachment protein receptor (SNARE)[1] proteins and large tethering complexes such as the exocyst (for review, see refs *1*−*3*). The SNARE proteins, present on either the vesicle (v-SNARE) or the target membrane (t-SNARE), are central to the membrane fusion process (*4*−*7*). Pairing of cognate v- and t-SNAREs into SNARE complexes brings the two apposed membranes into close proximity, facilitating fusion of the lipid bilayers. Although SNAREs are localized to distinct intracellular compartments, evidence suggests that they may not be sufficient to confer the necessary targeting specificity (*8*−*10*). In addition to the SNAREs, each step in membrane trafficking utilizes a unique hetero-oligomeric tethering complex and/or a long dimeric coiled-coil tethering protein (*2*, *11*). These tethering proteins interact with vesicle and target membrane proteins to physically link the membranes. It is this combination of both tethering and subsequent SNARE-mediated docking that leads to specific vesicle targeting.

In exocytosis, secretory vesicles are tethered to the plasma membrane by an evolutionarily conserved protein complex called the exocyst (Sec6/8 complex; *12*, *13*). The complex consists of eight proteins: Sec3p, Sec5p, Sec6p, Sec8p, Sec10p, Sec15p, Exo70p, and Exo84p (*12*, *14*). In yeast, the exocyst localizes to the tip of the growing bud and to the mother-daughter neck before cytokinesis. Phenotypic analysis of yeast temperature-sensitive mutants indicates that the exocyst is required for secretory vesicle fusion, at a step prior to exocytic SNARE complex assembly (*15*−*17*). Similarly, the exocyst is found at sites of active exocytosis and membrane expansion in mammalian cells, where it is required for neurite outgrowth (*18*, *19*), transport of basolateral cargo in polarized epithelial cells (*20*, *21*), and insulin-stimulated GLUT4 vesicle trafficking (*22*). In *Drosophila*, it has been shown to be required for neurite extension (*23*), as well as establishment of oocyte polarity (*24*). The exocyst also shares functional homology with tethering complexes that regulate other intracellular trafficking pathways (*2*).

† This work was supported by start-up funds from the University of Massachusetts Medical School to M.M. and an award from the American Heart Association to M.V.S.S.

* To whom correspondence should be addressed: Department of Biochemistry and Molecular Pharmacology, University of Massachusetts Medical School, Worcester, MA 01605. Telephone: 508-856-8318. Fax: 508-856-6464. E-mail: mary.munson@umassmed.edu.

[1] Abbreviations: CD, circular dichroism; DTT, dithiothreitol; GST, glutathione-*S*-transferase; MW, molecular weight; PMSF, phenylmethyl sulfonyl fluoride; SNARE, soluble *N*-ethylmaleimide sensitive factor attachment protein receptor; TCEP, Tris(2-carboxyethyl)phosphine hydrochloride; t-SNARE, target membrane SNARE protein; v-SNARE, vesicle SNARE protein.

10.1021/bi048008z CCC: $30.25
Published on Web 04/02/2005

The exocyst complex may also regulate SNARE complex assembly and subsequent membrane fusion. Previously, we showed that an N-terminal domain of the t-SNARE Sso1p inhibits binding of its C-terminal SNARE motif to the partner t-SNARE Sec9p (*25*−*27*). We hypothesized that this inhibition functioned to impart spatial and temporal control on exocytosis and would be released by a regulator(s) ("opener") localized to sites of secretion. Members of the exocyst complex are excellent candidates for regulators of the SNARE complex formation: they are properly localized, show genetic interactions with the SNAREs, and their temperature-sensitive phenotypes are consistent with a role prior to SNARE complex assembly (*15*−*17*, *28*−*31*). However, no direct interaction had previously been detected between the SNAREs and any of the exocyst subunits.

Characterization of the individual exocyst subunits has been obtained through genetic approaches in yeast, two-hybrid analyses, and co-immunoprecipitations of *in vitro* translated, radiolabeled components (*14*, *32*, *33*). In yeast, the exocyst subunit Sec15p associates with secretory vesicles through interactions with the Rab family GTPase Sec4p (*32*). The complex is localized to sites of exocytosis at the bud tip and mother-bud neck, likely through the interactions of Sec3p and Exo70p with Rho family GTPases (*34*). Sec5p is likely to be the structural core of the complex, because it interacts with five of the other subunits (*14*, *32*). Little is known about the functions of the remaining subunits, including Sec6p (*35*). The co-immunoprecipitation experiments revealed interactions between Sec6p and both Sec5p and Sec8p (*32*), but further characterization had not been done.

Here, we describe the biochemical and biophysical properties of the yeast exocyst subunit Sec6p. Purified Sec6p is a helical dimeric protein and contains a well-folded C-terminal domain. A 111-amino acid sequence located between the N- and C-terminal domains is important for dimerization. Moreover, we show that the Sec6p dimer directly binds the t-SNARE Sec9p and inhibits Sec9p from binding its cognate t-SNARE, Sso1p. These data suggest a role for Sec6p and therefore the rest of the exocyst complex in the regulation of SNARE complex assembly and membrane fusion.

EXPERIMENTAL PROCEDURES

Protein Expression and Purification. Genes encoding full-length Sec6p (1−805) and the various truncations were amplified by polymerase chain reaction and cloned into the *Nde*I and *Bam*HI sites of pET15b vector (Novagen), which introduced a 6-histidine tag (His_6) at their N termini. All constructs were confirmed by sequencing.

All proteins were expressed in *Escherichia coli* BL21(DE3) cells. To maximize protein solubility, cells were grown at 37 °C in Luria Bertani medium to an OD at 600 nm of 0.3−0.4. Cells were shifted to 20 °C until the OD_{600} reached 0.6−0.8. Protein expression was induced with 0.1−0.3 mM isopropyl-β-D-thiogalactoside, and cells were grown for 3 h more at 20 °C. Cells were harvested and frozen at −80 °C until lysis. His_6-tagged proteins were purified using nickel NTA resin (Qiagen). β-Mercaptoethanol (5 mM) or dithiothreitol (DTT, 1 mM) was used in all buffers. Full-length His_6-Sec6p, His_6-Sec6CT1 (amino acids 300−805), and His_6-Sec6CT2 (amino acids 411−805) were further purified on a MonoQ 10/10 anion-exchange column (Amersham Pharmacia Biotech) in a 20 mM Tris buffer at pH 8 using linear gradients of 200−400, 100−500, or 200−400 mM NaCl, respectively. Each protein was subsequently run on a Superdex 200 16/60 gel filtration column (Amersham Pharmacia Biotech) in KPhos buffer (10 mM potassium phosphate at pH 7.4 containing 140 mM KCl and 1 mM DTT, unless otherwise specified). Fractions were run on SDS−PAGE and stained with Coomassie blue. Those fractions containing >95% pure protein were pooled. The majority of the biophysical studies were performed with the His_6 affinity tag attached. For some experiments, however, the His_6 tag was removed by thrombin protease cleavage, followed by MonoQ anion-exchange chromatography. Proteins were concentrated using centrifugal spin concentrators (Millipore). Protein concentrations were determined either by measuring the absorbance at 280 nm or by a ninhydrin protein assay (*36*). Proteins were frozen in KPhos buffer containing 10% glycerol at −80 °C. The yield of each protein was generally 0.5−2 mg/L of bacterial cell culture. All of the purified proteins were soluble to ≥2 mg/mL, with no detectable aggregation.

The cytoplasmic regions of the SNARE proteins Sso1p, Snc2p, and Sec9p were purified as described (*25*). For all experiments, we used the C-terminal SNAP-25 homologous domain of Sec9p (residues 416−651; referred to as Sec9p); this domain has been shown to be fully functional *in vivo* (*29*).

Analytical Gel Filtration. Experiments were performed on either a Superdex 200 10/30 or Superose 6 10/30 column (Amersham); both have a bed volume of 24 mL. Proteins at varying concentrations (typically 100−200 μL of 1−10 μM) were loaded onto the column pre-equilibrated in KPhos buffer containing 1 mM DTT, and eluted peaks were observed by monitoring the absorbance at 280 nm. Each run was repeated at least 3 times. The gel filtration columns were calibrated using standards (thyroglobulin, 670 kD; γ-globulin, 158 kD; ovalbumin, 44 kD; myoglobin, 17 kD; Bio-Rad).

For examination of Sec6p in yeast lysates, BY4741 cells (*MAT***a** *his3*Δ*1 leu2*Δ*0 met15*Δ*0 ura3*Δ*0*; Invitrogen) were grown in rich media to an OD_{600} of 0.8−1.0 and spheroplasts were prepared from 150 OD_{600} units of cells as modified from ref *37*. Cells were harvested, washed in 50 mL ice-cold washing buffer (10 mM Tris at pH 7.4, and 10 mM NaN_3), and resuspended in 15 mL spheroplasting buffer (50 mM $NaPO_4$ at pH 7.4, 1.4 M Sorbitol, 35 mM β-mercaptoethanol, 10 mM NaN_3, and 100 μg/mL Zymolyase T-100). These were incubated at 30 °C for 30 min, layered on top of a 15 mL 1.5 M sorbitol solution (50 mM $NaPO_4$ at pH 7.4, 1.5 M Sorbitol, 10 mM NaN_3, and protease inhibitors), and centrifuged through the sorbitol cushion for 10 min at 1000*g*. The pellets were resuspended in 0.6 mL cold lysis buffer (20 mM PIPES at pH 6.8, 100 mM NaCl, 1 mM EDTA, 1% NP-40, 1 mM DTT, and protease inhibitors). The lysates were cleared by centrifugation for 10 min at 10000*g*, and 200 μL aliquots were loaded onto the Superose 6 gel-filtration column in lysis buffer with 0.1% NP-40. The fractions from three runs were collected and precipitated with trichloroacetic acid. The presence of Sec6p in the fractions was determined by immunoblot analysis using α-Sec6p antibody.

Immunoblot Analyses. Antiserum against purified Sec6p was generated by the Pocono Rabbit Farm and Laboratory Inc. The antiserum was affinity-purified using recombinant Sec6p coupled to CNBr-activated sepharose resin (Amersham). Proteins were separated by SDS−PAGE, transferred to nitrocellulose membrane, and probed by Western blot analysis using the affinity-purified α-Sec6p antibodies. The blots were developed using peroxidase-conjugated anti-rabbit secondary antibodies (Roche) and enhanced chemiluminescent detection (ECL; Amersham); the total density of each band was determined using a Bio-imaging EPI Chemi II Darkroom (UVP) and Labworks 4.0 software.

Circular Dichroism (CD) Spectroscopy. CD spectra were recorded on a J810 spectropolarimeter (Jasco) fitted with a Peltier-type temperature controller. The protein concentrations for the various samples were between 4 and 10 μM in KPhos buffer containing 5 mM Tris(2-carboxyethyl)phosphine hydrochloride (TCEP). All spectra were recorded as an average of three scans from 200 to 270 nm, in a 1 mm path-length quartz cuvette (Hellma). For each spectrum, the minimum at 222 nm was used to estimate the mean residue ellipticity and percent helicity. Thermal transitions were performed at the rate of 1 °C per minute while monitoring ellipticity at 222 nm. All CD experiments, both wavelength spectra and thermal melts, were performed at least 3 times.

Equilibrium Analytical Ultracentrifugation. The purified protein constructs were dialyzed into KPhos buffer; the protein concentrations ranged between 0.45 and 5.2 μM (for His_6-Sec6p) and 0.30 and 7.8 μM (for Sec6CT1). The proteins were centrifuged to equilibrium at a range of speeds between 10 000 and 18 000 rpm in an Optima XLI analytical ultracentrifuge (Beckman) at 4 °C (verified when consecutive scans acquired in 2 h intervals were superimposable). The absorbance at 230 or 280 nm was measured, depending on the absorbance spectra of the individual samples. At least nine data sets each (minimum of 3 protein concentrations at 3 speeds) were analyzed by nonlinear least-squares fitting using WinNonlin software (version 1.06, University of Connecticut), and the partial specific volume of the sample and density of the buffer were calculated by SednTerp (version 1.08, University of New Hampshire). Sec6p data sets were globally best-fit to a single species with an apparent molecular weight of 197 000 D ± 12 500 SEM [calculated molecular weight (MW) of the Sec6p dimer = 191 000]. The Sec6CT1 data sets fit poorly to either a monomer or a dimer model and were globally best-fit by a reversible monomer−dimer model. Visual inspection of the deviations of the residual plots, as well as the square root of variance for the fits, indicated that the monomer−dimer model was a better fit than either monomer−trimer, monomer−tetramer, or higher order oligomer models.

Limited Proteolysis. Aliquots of Sec6p (5 μg) were incubated with either trypsin or thermolysin at room temperature for 30 min. Reactions contained either 0.1, 0.2, 0.5, or 1 μg of each protease. Buffer conditions used for digestion were 10 mM Tris at pH 8.0, 150 mM NaCl, 10% glycerol, 10 mM $CaCl_2$, and 1 mM DTT. After incubation, the digests were boiled for 5 min in sample-loading buffer, run on a 10% SDS polyacrylamide gel, and transferred to a poly(vinylidene difluoride) membrane. Protein bands were visualized by staining with Ponceau S. The region of the membrane containing the band of interest was cut out and subjected to N-terminal sequencing by Edman degradation (Tufts University).

Glutathione-S-transferase (GST) Pull-Down Assays. GST and GST-tagged proteins were purified using glutathione agarose affinity chromatography. Protease inhibitor cocktail tablets (Roche) were necessary during the lysis, and extra phenylmethyl sulfonyl fluoride (PMSF) was added every 2 h. The purified proteins immobilized on glutathione beads were subsequently washed in KPhos buffer containing 0.05% NP-40, protease inhibitors, and 1 mM PMSF. Purified soluble proteins were added to the immobilized GST-tagged proteins, and the mixtures (~2−10 μM each protein) were incubated for 1 h at 4 °C with mixing to allow binding. The beads were centrifuged, and the supernatants were removed. The beads were washed 3 times with KPhos buffer containing 0.05% NP-40. Equal volume aliquots of the supernatants and beads were analyzed by SDS−PAGE and stained with Coomassie blue.

SNARE Assembly Assays. Protein samples (10 μM each) were incubated in KPhos buffer for 0−72 h at 18 °C. For the gel-mobility shift assay, samples were run on 1.5 mm 6% native polyacrylamide gels (37.5:1 acrylamide/bis) at 4 °C for 1.25 h at 30 mA. Gels were buffered at pH 7.4 using 43 mM imidazole and 35 mM HEPES and stained with Coomassie blue. For the gel filtration assay, 200 μL of each sample was loaded on the Superose 6 10/30 column pre-equilibrated in KPhos buffer and the absorbance was monitored at 280 nm. Quantitation of the free Sso1p peak and analyses of the assembly kinetics were performed as described previously (*25*).

RESULTS

Sec6p Is a Dimer. Sec6p was overexpressed in *E. coli* with an N-terminal His_6 tag and purified by Ni^{2+} affinity, anion-exchange, and gel filtration chromatography to obtain >95% pure protein. The secondary structural content and thermal stability of Sec6p were analyzed by CD spectroscopy. The CD spectrum revealed a predominantly α-helical protein (~48% helical; Figure 1A; *38*). By monitoring the ellipticity (θ) at 222 nm as a function of the temperature, we determined that Sec6p is only moderately stable, with a melting point near 36 °C. Its thermal denaturation was irreversible due to precipitation at temperatures >40 °C, precluding quantitative analysis of its thermal stability (data not shown).

When the oligomeric state of Sec6p was examined using an analytical Superdex 200 10/30 gel filtration column, it displayed a significantly larger apparent MW than expected from its calculated MW. The eluted protein was monodisperse, having only a single symmetrical peak with an apparent MW of 180 kD (calculated MW = 95 kD; data not shown). Two possibilities are consistent with these data: Sec6p is either a dimer or a monomer with a significantly elongated shape.

To differentiate between these possibilities, we performed equilibrium analytical ultracentrifugation experiments (Figure 1B). Multiple concentrations of Sec6p (0.45−5.2 μM) were centrifuged to equilibrium at three different speeds (10, 12, and 14 krpm). At all speeds and concentrations tested, the data were globally best-fit to a dimer (apparent MW = 197 kD; calculated MW of the Sec6p dimer = 191 kD). We also could not detect any monomeric Sec6p by gel filtration;

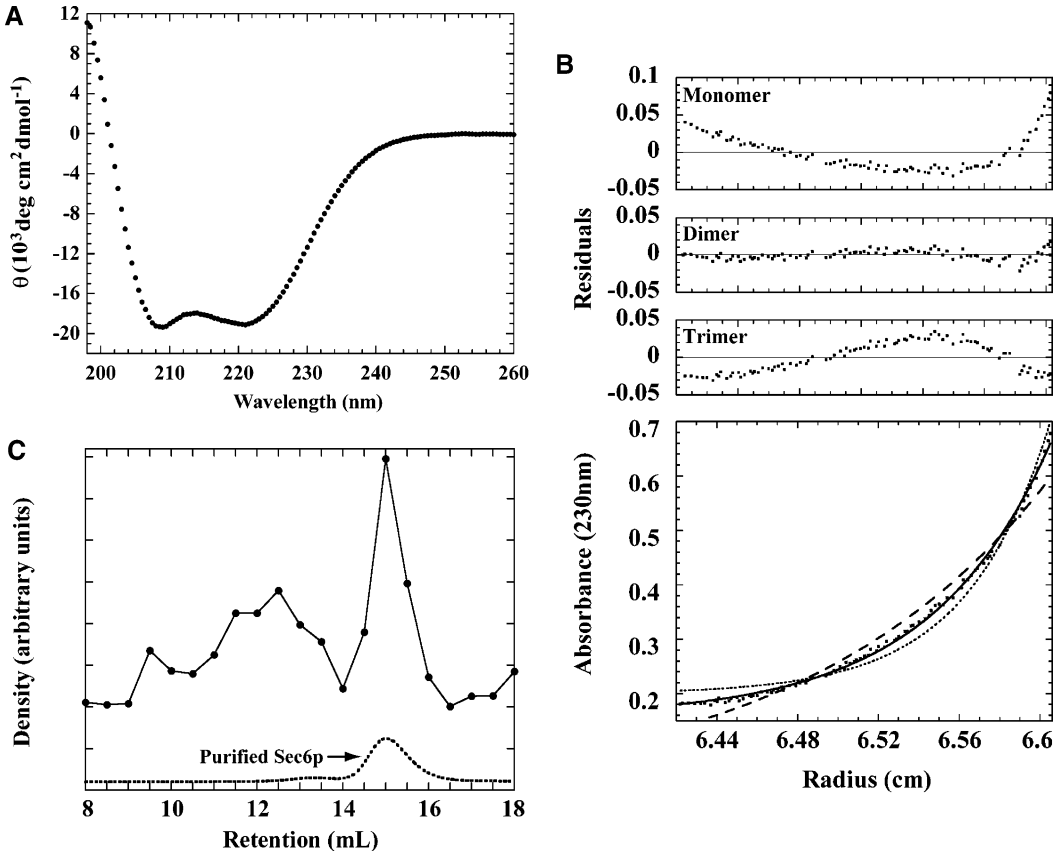

FIGURE 1: Sec6p is a helical dimer. (A) Sec6p was analyzed by CD. The CD wavelength spectrum was obtained at 5 μM Sec6p at 4 °C. The characteristic minimum at 222 nm was indicative of ~48% helicity. (B) Representative sedimentation equilibrium ultracentrifugation data for Sec6p. Sec6p (1 μM) was centrifuged to equilibrium at 12 000 rpm (lowest panel). A solid line (—) represents a global least-squares fit to a dimer model; global fits to monomer (- - -) and trimer (•••) models are shown for comparison. The corresponding residuals are shown in the upper panels. (C) Sec6p from yeast lysates was analyzed by Superose 6 gel filtration chromatography (—). Fractions from the column were analyzed by SDS−PAGE and α-Sec6p antibody immunoblots. The plot indicates quantitative densitometry of the Sec6p bands. The purified recombinant Sec6p is shown below as a marker for the dimer (- - -).

therefore, we set an upper limit for the dissociation constant K_d at ≤0.1 μM. Removing the His_6 tag did not affect dimerization (data not shown).

We next determined whether Sec6p was a dimer *in vivo*. Wild-type yeast cells were lysed, and the cleared lysate was loaded on a Superose 6 10/30 gel filtration column (Figure 1C). We observed two peaks of Sec6p in immunoblots of the eluted fractions. The first peak elutes with an apparent MW of ~800 kD, consistent with Sec6p assembled into the exocyst complex. The second peak elutes with an apparent molecular weight similar to recombinant dimeric Sec6p (apparent MW = 180 kD). These data suggest that *in vivo* Sec6p exists in two pools: assembled into the exocyst complex and free dimer. These data, however, did not rule out the possibility that Sec6p may also be dimeric when present in the exocyst complex. Because the ratio of the Sec6p peaks (exocyst complex versus free dimer) varied greatly with the lysis conditions, we did not attempt to quantitate the amount of free Sec6p *in vivo*.

Sec6p Contains an Independently Folded C-Terminal Domain. Because Sec6p is a 93-kD protein, we hypothesized that it might be comprised of several independently folded structural domains. To identify these domains and to map the region(s) important for dimerization, we performed limited proteolysis experiments. Purified Sec6p protein was digested using a range of concentrations of trypsin, chymotrypsin, proteinase K, and thermolysin. These digests were analyzed by SDS−PAGE for smaller fragments that were resistant to cleavage by several concentrations of at least two of the proteases. Two such fragments (~45 and ~60 kD) were identified in both the trypsin and thermolysin digests (Figure 2A). N-Terminal sequencing identified the tryptic fragments as C-terminal domains beginning at amino acids 292 and 408. These domains comprise approximately $^2/_3$ and $^1/_2$ of full-length Sec6p, respectively. The apparent molecular weights on the SDS−PAGE gel suggested that the C-terminal end of each fragment coincided with the end of the protein.

For the longer C-terminal fragment, secondary structure predictions suggested that residues 292−299 might be unstructured (*39*); therefore, we expressed and purified a construct containing residues 300−805, called Sec6CT1. Purified Sec6CT1 eluted as two peaks in gel filtration experiments (Figure 2B). The retention volume of the peaks indicated that Sec6CT1 formed both a monomer and a higher molecular weight oligomer (apparent MW = 76 and 260 kD; calculated MW = 61 kD). The monodispersity of the oligomeric peak, as well as the fact that the monomer and oligomer showed a reversible equilibration, indicated that this peak was not due to nonspecific aggregation. This monomer−oligomer equilibration was slower than the duration of the gel filtration run (≥30 min). From our gel filtration data, we estimate the K_d to be at least 10-fold weaker than for the full-length dimer. Because the full-length Sec6p is dimeric, we expected that the higher molecular

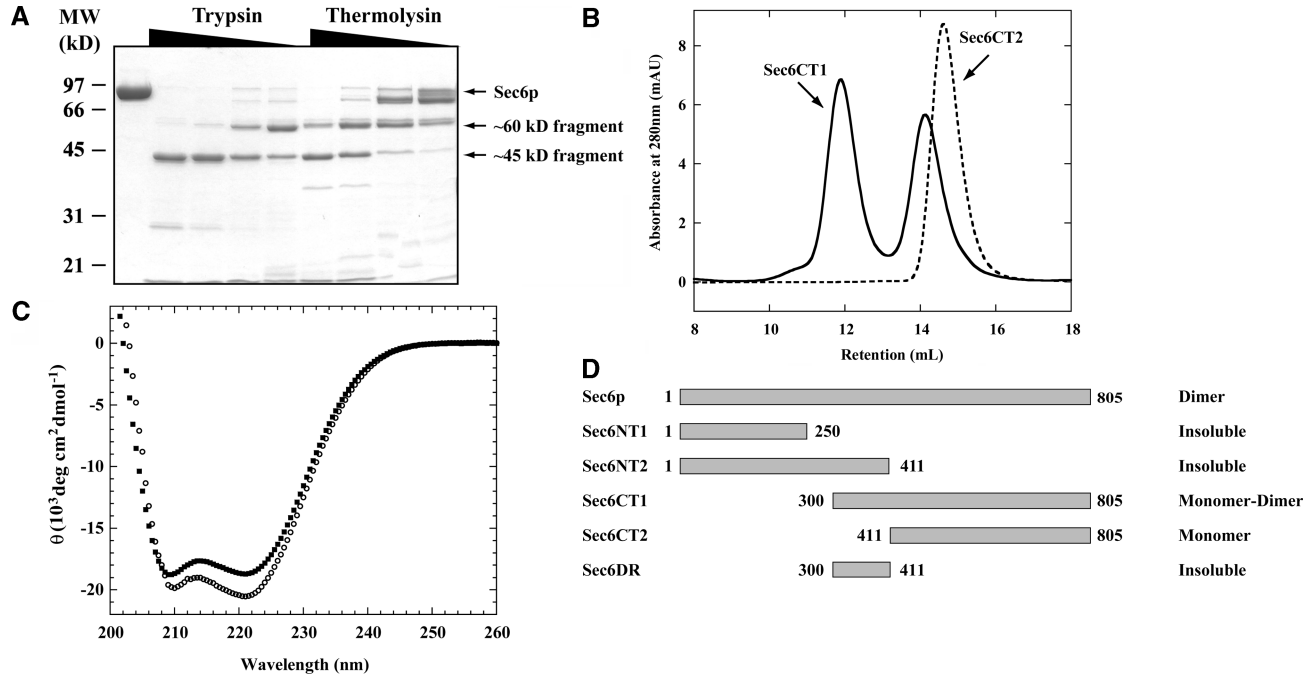

FIGURE 2: Identification and characterization of the C-terminal domain of Sec6p and the dimerization region. (A) Folded structural domains of Sec6p were mapped by limited proteolysis. Purified Sec6p was incubated with decreasing concentrations of trypsin or thermolysin for 30 min at room temperature. The digests were boiled for 5 min in SDS−PAGE loading buffer, run on a 12% SDS−PAGE gel, and Coomassie-stained. The mobilities of Sec6p and the C-terminal fragments are marked on the right. (B) Oligomeric states of recombinant Sec6CT1 (—) and Sec6CT2 (- - -) were analyzed by Superdex 200 gel filtration chromatography. For each protein, 200 μL of 5 μM solution was loaded. (C) Sec6CT1 (■) and Sec6CT2 (○) were analyzed by CD. Only the dimer of Sec6CT1 is shown; the results from the monomer were indistinguishable from the dimer. CD wavelength spectra were obtained at a 5 μM protein concentration and 4 °C. (D) Schematic diagram of the N- and C-terminal constructs of Sec6p are depicted. Numbers indicate the first and last amino acid of each construct. The observed oligomerization states are presented on the right.

weight oligomer of Sec6CT1 would also be dimeric; indeed, results from equilibrium analytical ultracentrifugation experiments are consistent with a monomer−dimer model (data not shown). The dimeric form of Sec6CT1 eluted earlier than full-length Sec6p on the Superdex 200 column. This indicated that Sec6CT1 has a slightly larger hydrodynamic radius than Sec6p, suggesting a significant deviation from an ideal spherical shape. From these data, we conclude that this C-terminal domain contains the dimerization region and the N-terminal domain is necessary for stability of the dimeric form.

The monomer and dimer of Sec6CT1 were separated by gel filtration, and their secondary structure and stability were examined by CD. These experiments indicated that both forms are folded (~52% helical; Figure 2C; only the dimer is shown). Both the monomer and dimer were slightly more thermally stable than full-length Sec6p; the melting temperatures were ~42 °C (data not shown). Both conformations showed a single melting transition, although their melts were irreversible. Because the monomer and dimer have the same molar ellipticity and thermal stability when analyzed at the same protein concentration, this suggests that the α-helical content and stability of the monomeric species does not significantly change upon dimerization.

Identification of the Dimerization Region. The shorter C-terminal construct Sec6CT2 (411−805) was purified. CD experiments indicated that it was also well-folded, with ~59% helicity (Figure 2C). Its thermal denaturation indicated a melting temperature of ~46 °C but was also irreversible (data not shown). Unlike both Sec6p and Sec6CT1, Sec6CT2 was shown by gel filtration to be completely monomeric at concentrations up to 1 mM (Figure 2B; apparent MW = 47 kD; calculated MW = 48 kD). On the basis of these results, we conclude that Sec6CT2 comprises a folded structural core domain and that the region between amino acids 300 and 410 (Sec6DR) is important for dimerization (Figure 2D).

By comparing the mean residue helicities of full-length Sec6p to that of the CT1 and CT2 domains, we calculated that the corresponding N-terminal regions should be approximately 40% helical when present in the full-length protein. The dimerization region (300−410) was calculated to be ~30% helical. To test these predictions, we cloned the N-terminal truncations 1−250 and 1−410 and the dimerization region. All three proteins expressed well but were completely insoluble, precluding any biophysical characterization.

Sec6p Interacts with the t-SNARE Sec9p and Inhibits SNARE Complex Assembly. We next examined whether purified Sec6p could interact with the yeast exocytic SNARE proteins: Sso1p, Sec9p, or Snc2p. These proteins are the yeast homologues of syntaxin, SNAP-25, and VAMP/synaptobrevin, respectively. We tested each interaction using GST-tagged pull-down experiments. Sec6p interacted specifically with the t-SNARE Sec9p and not GST alone (Figure 3A). Sec6p did not bind to the t-SNARE Sso1p and bound relatively weakly to the v-SNARE Snc2p (Figure 3B). Because Sso1p forms an inhibited "closed" conformation (*25*, *26*), we used a GST-Sso1CTB (residues 179−265) construct to test if Sec6p would interact with the SNARE motif of Sso1p; no interaction was detected (Figure 3C). In each case, the GST pull-down results were confirmed by gel filtration experiments (data not shown).

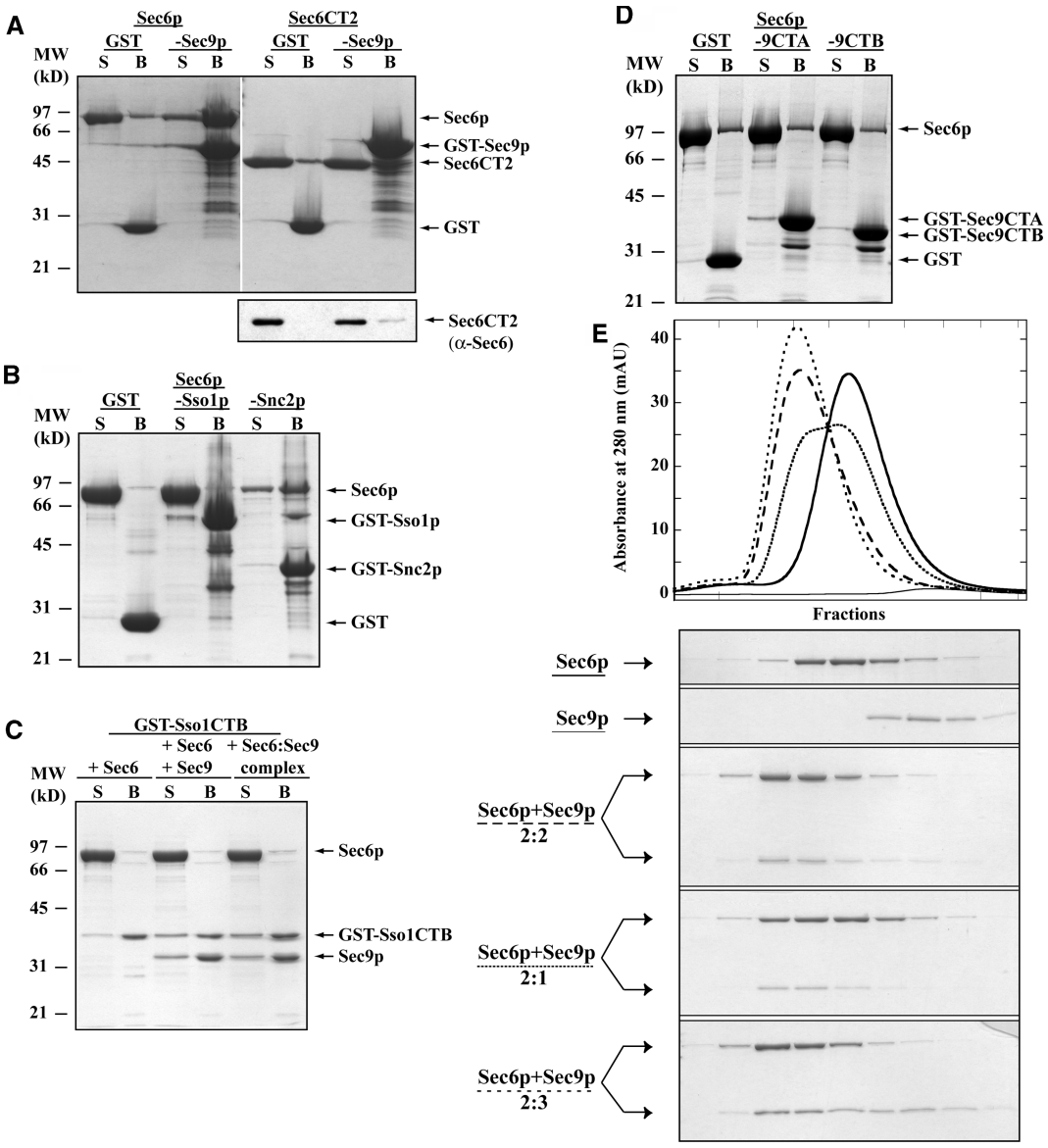

FIGURE 3: Dimer of Sec6p binds the t-SNARE Sec9p. (A) GST and GST-Sec9p were immobilized on glutathione agarose beads and incubated for 1 h at 4 °C with an equimolar amount of Sec6p or Sec6CT2. Equivalent amounts of supernatant (S) and bead (B) fractions were analyzed on Coomassie-stained SDS−PAGE gels. The mobilities of the various proteins are marked with arrows on the right. Additional bands in the GST-Sec9p lanes are GST-Sec9p proteolysis fragments. Because this proteolysis of GST-Sec9p made detection of bound Sec6CT2 difficult, we used Western blot analysis using α-Sec6p antibody to detect the Sec6CT2 (lower panel). Lanes marked as "-Sec9p" denote that the GST-Sec9p construct was used. Similar labels were used for Sso1p, Snc2p, Sec9CTA, and Sec9CTB. (B) GST-Sso1p and GST-Snc2p were tested for interaction with Sec6p. Sec6p weakly binds Snc2p and thus readily dissociates during the washing steps. (C) GST-Sso1CTB (179−265) out competes Sec6p for binding to Sec9p. Immobilized GST-Sso1CTB was mixed with either Sec6p alone (+Sec6), with Sec6p and Sec9p simultaneously (+Sec6+Sec9), or with pre-formed Sec6p−Sec9p complex (+Sec6:Sec9 complex). (D) GST-Sec9CTA (416−504) and GST-Sec9CTB (571−651) were tested for interaction with Sec6p. (E) Five separate Superose 6 gel filtration profiles showing Sec6p binding to Sec9p (top graph; curves are marked on the left): purified Sec6p (10 μM), purified Sec9p (10 μM), and Sec6p+Sec9p at 2:2 (10 μM each), 2:1 (10 μM Sec6p and 5 μM Sec9p), and 2:3 (10 μM Sec6p and 15 μM Sec9p) ratios, respectively. Fractions (0.5 mL) were collected, run on SDS−PAGE gels, and Coomassie-stained (below). Note that the molar extinction coefficient at 280 nm for Sec9p is 30-fold less than for Sec6p.

To identify the regions of Sec6p and Sec9p that interact with each other, we tested binding of the C-terminal domains of Sec6p to Sec9p in both GST pull-down and gel filtration experiments. Sec9p did not interact with either Sec6CT1 or Sec6CT2 (Figure 3A; Sec6CT2 is shown). These data suggested that the N-terminal domain of Sec6p is necessary for interactions with Sec9p. In addition, we expressed GST fusions of both SNARE motifs of Sec9p (residues 416−504 and 571−651) and did not detect binding of Sec6p to either of these constructs (Figure 3D). The construct containing the intervening loop region (505−570) was extremely susceptible to proteolysis during purification and could not be definitively tested for binding to Sec6p.

Using a series of gel filtration experiments at different protein concentrations, we estimated that the affinity for Sec6p and Sec9p is in the high nanomolar range (500 nM−1 μM; data not shown); this is only an estimate, however, because the complex is continuously diluted while it migrates through the gel filtration column. We tested the ability of Sec6p to compete with the binding of Sec9p to its partner t-SNARE Sso1p using the GST-Sso1CTB construct (Figure 3C; 10 μM each). When Sec6p and Sec9p were

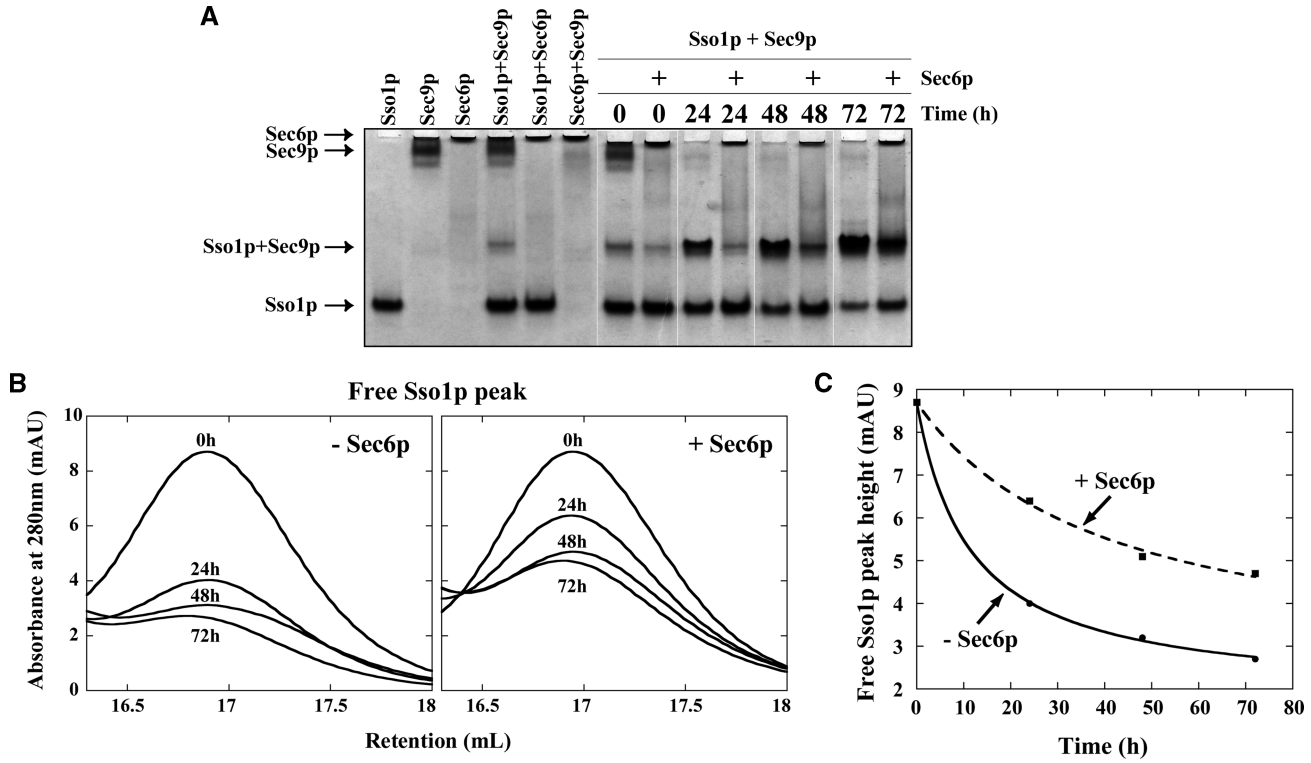

FIGURE 4: Sec6p inhibits t-SNARE complex assembly. (A) SNARE complex assembly was analyzed by a native gel mobility shift assay. Purified proteins were run as markers and are indicated at the top. The time course shows SNARE assembly ± Sec6p. Sso1p and Sec9p (10 μM each) were mixed together, ±10 μM Sec6p, and incubated at 18 °C for the times indicated. The mixtures were run on a 6% nondenaturing polyacrylamide gel and stained with Coomassie blue. The mobilities of the various proteins and complexes are marked on the left. Sec6p, which is a 190-kD dimer, does not migrate far into the top of the native gel. (B) SNARE complex assembly was monitored by Superose 6 gel filtration chromatography. Gel filtration profiles of 10 μM mixtures of Sso1p + Sec9p ± Sec6p were incubated at 18 °C for the times indicated. The region containing Sec6p and the SNARE complex is not shown to depict the free Sso1p peaks to scale. No absorbance outside of these regions was observed. (C) Quantitative analyses of the free Sso1p peaks as a function of time. The data were fit to a second-order rate equation; the rate constants obtained at 10 μM protein concentration were 2.4 M^{-1} s^{-1} in the absence of Sec6p (●, —) and 0.69 M^{-1} s^{-1} in the presence of Sec6p (■, - - -).

added to Sso1CTB simultaneously, all of the Sec9p bound to Sso1CTB. When we preformed the Sec6p−Sec9p complex and added it to Sso1CTB, we observed that all of the Sec9p dissociated from Sec6p and bound to Sso1CTB, indicating that the affinity of Sso1CTB for Sec9p is significantly tighter.

We also used gel filtration experiments to investigate the stoichiometry of the Sec6p−Sec9p complex. On the Superose 6 10/30 gel filtration column, the complex between Sec6p and Sec9p migrates with an apparent molecular weight that is consistent with a dimer of Sec6p bound to at least one copy of Sec9p (Figure 3E; 270 kD). When different ratios of protein concentrations were tested, a 2:2 Sec6p/Sec9p molar ratio resulted in complex formation, addition of Sec9p to a 2:3 ratio resulted in the complex plus excess Sec9p, while addition of less Sec9p (2:1) resulted in the complex plus excess Sec6p. These data indicate that the complex has a 2:2 stoichiometry; i.e., the dimer of Sec6p binds two molecules of Sec9p.

We used CD to monitor whether Sec9p folds when it interacts with Sec6p. Previous studies demonstrated that the interaction between Sec9p and Sso1p produced a significant increase in α-helicity as the SNARE motifs fold (*25*, *40*). We reasoned that Sec9p might also fold upon binding to Sec6p, increasing the total percent helicity. However, this was not observed. The CD signal of the Sec6p−Sec9p complex was not significantly different from a theoretical noninteracting combination of Sec6p and Sec9p (data not shown).

What is the role of Sec6p and the Sec6p−Sec9p interaction in SNARE complex assembly? One possibility is that Sec6p, through its interaction with Sec9p, might stimulate SNARE complex formation at sites of secretion. To test this hypothesis, we added purified Sec6p to our *in vitro* SNARE assembly assay (*25*, *26*). In this assay, purified Sso1p was incubated with Sec9p for different lengths of time at 18 °C, in the presence or absence of Sec6p. The resulting mixtures were run on a native protein gel, which separated the individual proteins from the SNARE complex (Figure 4A). Interestingly, we discovered that SNARE complex assembly was strongly inhibited by Sec6p. The Sec6p−Sec9p interaction decreased the rate of Sec9p binding to Sso1p.

Moreover, similar results were observed when the mixtures were separated by Superose 6 gel filtration chromatography (Figure 4B). Because the peaks for Sec6p, Sec9p, and the Sso1p−Sec9p complex overlapped, we quantitated the rate of Sso1p−Sec9p complex assembly by monitoring the loss of free Sso1p, as described previously (Figure 4C; *25*). Consistent with previously published data, the rate constant for Sso1p−Sec9p complex formation was 2.4 M^{-1} s^{-1} in the absence of Sec6p. In the presence of Sec6p, the rate constant for SNARE complex assembly was 0.69 M^{-1} s^{-1}.

These data indicate that Sec6p, through its interaction with Sec9p, slows the rate of Sso1p−Sec9p complex formation by ~3.5-fold.

DISCUSSION

To elucidate the function of the exocyst in vesicular trafficking, biophysical and structural characterization of the exocyst proteins is necessary. Here, we report the expression and purification of the yeast exocyst protein Sec6p and show that it is a folded α-helical dimer containing an independently folded C-terminal domain. We have mapped the region responsible for dimerization to the 111 residues preceding this domain. Moreover, we have observed a direct interaction between a yeast exocyst subunit and an exocytic SNARE protein: Sec6p binds to the plasma membrane t-SNARE Sec9p. Significantly, this Sec6p−Sec9p interaction inhibits the rate of SNARE complex assembly.

The independently folded C-terminal domain of Sec6p is composed of residues 411−805. When expressed and purified, this domain was found to be completely monomeric. Inclusion of residues 300−410 caused the domain to dimerize. This construct, however, had a lower binding affinity than the full-length Sec6p, implicating the N-terminal region in dimer stabilization. The dimerization region (300−410), which was calculated to be folded in the full-length protein, was found to be insoluble when expressed by itself. An analysis of the protein sequence by database searches did not suggest significant homology with any previously characterized domains, and the region is not predicted to form a coiled coil. Unfortunately, our attempts to characterize the N-terminal domain were also thwarted by its insolubility. It is likely that the N-terminal region makes important contacts with the C-terminal domain. These NT−CT contacts would be necessary for proper folding and/or stability of the N-terminal region, without significantly altering the structure and stability of the C-terminal domain.

The dimerization of Sec6p was unexpected based on previous stoichiometry measurements. Novick and colleagues used ^{35}S-methionine labeling to quantitate the amount of each subunit in the exocyst complex, as well as Sec8p-myc immunoprecipitation experiments, to conclude that the complex had one copy of each subunit (*12*). Fractionation experiments, however, suggested that at least two pools of Sec6p are present in cells (Figure 1C; *35*); several of the other exocyst subunits show a similar distribution (*14*, *41*, *42*). Their distribution is likely due to the fact that the exocyst undergoes repeated rounds of assembly and disassembly during the cell cycle. This was recently demonstrated by high-resolution video microscopy, which showed that the exocyst assembles at sites of secretion in a dynamic fashion (*31*). Our gel filtration results indicate that the free pool of Sec6p elutes with a homodimeric molecular weight. Dimerization might provide a mechanism to stabilize Sec6p when it is not assembled in the exocyst complex. Consistent with this idea, the C-terminal constructs, which do not form stable dimers *in vitro*, are readily degraded when expressed in yeast (data not shown).

Using GST pull-down assays and gel filtration chromatography, we discovered that the dimer of Sec6p binds to the t-SNARE protein Sec9p. The interaction is specific to Sec9p; we did not detect any significant interaction between Sec6p and either the t-SNARE Sso1p or the v-SNARE Snc2p. Because Sec6p is an obligate dimer, we were unable to test if Sec6p monomers are able to bind Sec9p. The C-terminal domains, which are not stable dimers, do not interact with Sec9p; however, it is unclear whether the N-terminal domain and/or dimerization are sufficient for binding.

This interaction between a tethering complex and a SNARE protein is not unique to the exocyst. Interactions of SNAREs with other tethers, including p115, EEA1, and the COG, GARP/VFT, and HOPS complexes, have been observed (*43*−*50*). It is likely that each of the tethering complexes plays a crucial role in regulating and/or localizing specific SNARE complex assembly. We demonstrated that Sec6p significantly inhibits assembly of the t-SNARE complex, Sec9p−Sso1p. Quantitation of the rate of assembly indicates that Sec6p inhibits the rate by ~3.5-fold.

Is the role of Sec6p to prevent Sso1p from binding Sec9p *in vivo*? A negative regulator would provide temporal and spatial control of SNARE complex assembly. Several reasons suggest that this is not the function of the Sec6p−Sec9p complex. First, we previously demonstrated that Sso1p is negatively regulated by its own N-terminal domain, making regulation by Sec6p redundant (*25*, *26*). Second, the affinity of Sso1p for Sec9p is estimated to be significantly tighter (<50 nM) than the Sec6p−Sec9p complex; however, this estimate is complicated by the fact that the SNARE complex is kinetically trapped from disassembly in the absence of NSF/SNAP and ATP (*40*, *51*, *52*). We directly tested the differences in affinity by observing that Sec6p does not successfully compete with the SNARE motif of Sso1p (Sso1CTB) for Sec9p binding. Third, if the role of Sec6p is to prevent SNARE complex assembly, it would be expected to co-localize with Sec9p. The localization of Sec9p is significantly different from Sec6p; Sec9p is broadly distributed across the plasma membrane, and not specifically localized to sites of secretion (*29*). In addition, negative regulation is not consistent with the *in vivo* role(s) of the exocyst. Yeast temperature-sensitive mutants demonstrate that the exocyst plays a positive role in SNARE complex assembly and membrane fusion (*17*). These mutants, including *sec6*−*4*, accumulate secretory vesicles and have decreased levels of ternary SNARE complexes. Thus, it is highly unlikely that Sec6p is a negative regulator of Sec9p *in vivo*.

We hypothesize that Sec6p is a component of the SNARE assembly machinery that will stimulate SNARE complex assembly at the correct time and place. Because we examined the Sec6p−Sec9p interaction in the absence of the partners of Sec6p, we may have captured a stable intermediate in the SNARE assembly pathway. Upon arrival of the secretory vesicle, the role of Sec6p would be to interact with Sec9p and, in conjunction with another regulatory protein(s), to drive Sec9p−Sso1p assembly and subsequent ternary SNARE complex formation and vesicle fusion. What is the other regulator(s)? Likely suspects are other exocyst subunits, such as Sec8p and Sec5p that directly interact with Sec6p (*32*). Alternatively, proteins such as Sec1p, which directly interact with the SNAREs and the exocyst complex (*37*, *53*), or an as yet unidentified regulator, such as the putative "opener" of Sso1p (*27*), are other potential candidates. Identification

of this regulator(s) will be a crucial step toward understanding the spatial and temporal regulation of membrane trafficking.

ACKNOWLEDGMENT

We are grateful to Dr. P. Novick for plasmids and helpful discussions. We are especially grateful to Dr. C. R. Matthews and his lab for use of the CD and for technical assistance. We thank Drs. C. Carr, F. Hughson, R. Gilmore, W. Kobertz, N. Rhind, and members of the Munson lab, for critical reading of this manuscript and advice. Thanks to C. Baldwin for editorial assistance.

REFERENCES

1. Brunger, A. T. (2001) Structural insights into the molecular mechanism of calcium-dependent vesicle-membrane fusion, *Curr. Opin. Struct. Biol. 11*, 163−173.
2. Whyte, J. R., and Munro, S. (2002) Vesicle tethering complexes in membrane traffic, *J. Cell. Sci. 115*, 2627−2637.
3. Ungar, D., and Hughson, F. M. (2003) SNARE protein structure and function, *Annu. Rev. Cell Dev. Biol. 19*, 493−517.
4. Sutton, R. B., Fasshauer, D., Jahn, R., and Brunger, A. T. (1998) Crystal structure of a SNARE complex involved in synaptic exocytosis at 2.4 Å resolution, *Nature 395*, 347−353.
5. Weber, T., Zemelman, B. V., McNew, J. A., Westermann, B., Gmachl, M., Parlati, F., Sollner, T. H., and Rothman, J. E. (1998) SNAREpins: Minimal machinery for membrane fusion, *Cell 92*, 759−772.
6. McNew, J. A., Parlati, F., Fukuda, R., Johnston, R. J., Paz, K., Paumet, F., Sollner, T. H., and Rothman, J. E. (2000) Compartmental specificity of cellular membrane fusion encoded in SNARE proteins, *Nature 407*, 153−159.
7. Tucker, W. C., Weber, T., and Chapman, E. R. (2004) Reconstitution of Ca^{2+}-regulated membrane fusion by synaptotagmin and SNAREs, *Science 304*, 435−438.
8. Fasshauer, D., Antonin, W., Margittai, M., Pabst, S., and Jahn, R. (1999) Mixed and non-cognate SNARE complexes. Characterization of assembly and biophysical properties, *J. Biol. Chem. 274*, 15440−15446.
9. Grote, E., and Novick, P. J. (1999) Promiscuity in Rab-SNARE interactions, *Mol. Biol. Cell 10*, 4149−4161.
10. Yang, B., Gonzalez, L., Jr., Prekeris, R., Steegmaier, M., Advani, R. J., and Scheller, R. H. (1999) SNARE interactions are not selective. Implications for membrane fusion specificity, *J. Biol. Chem. 274*, 5649−5653.
11. Guo, W., Sacher, M., Barrowman, J., Ferro-Novick, S., and Novick, P. (2000) Protein complexes in transport vesicle targeting, *Trends Cell Biol. 10*, 251−255.
12. TerBush, D. R., Maurice, T., Roth, D., and Novick, P. (1996) The Exocyst is a multiprotein complex required for exocytosis in *Saccharomyces cerevisiae*, *EMBO J. 15*, 6483−6494.
13. Hsu, S. C., Ting, A. E., Hazuka, C. D., Davanger, S., Kenny, J. W., Kee, Y., and Scheller, R. H. (1996) The mammalian brain rsec6/8 complex, *Neuron 17*, 1209−1219.
14. Guo, W., Grant, A., and Novick, P. (1999) Exo84p is an exocyst protein essential for secretion, *J. Biol. Chem. 274*, 23558−23564.
15. Salminen, A., and Novick, P. J. (1987) A ras-like protein is required for a post-Golgi event in yeast secretion, *Cell 49*, 527−538.
16. Finger, F. P., and Novick, P. (2000) Synthetic interactions of the post-Golgi sec mutations of *Saccharomyces cerevisiae*, *Genetics 156*, 943−951.
17. Grote, E., Carr, C. M., and Novick, P. J. (2000) Ordering the final events in yeast exocytosis, *J. Cell Biol. 151*, 439−452.
18. Hazuka, C. D., Foletti, D. L., Hsu, S. C., Kee, Y., Hopf, F. W., and Scheller, R. H. (1999) The sec6/8 complex is located at neurite outgrowth and axonal synapse-assembly domains, *J. Neurosci. 19*, 1324−34.
19. Vega, I. E., and Hsu, S. C. (2001) The exocyst complex associates with microtubules to mediate vesicle targeting and neurite outgrowth, *J. Neurosci. 21*, 3839−3848.
20. Grindstaff, K. K., Yeaman, C., Anandasabapathy, N., Hsu, S. C., Rodriguez-Boulan, E., Scheller, R. H., and Nelson, W. J. (1998) Sec6/8 complex is recruited to cell−cell contacts and specifies transport vesicle delivery to the basal-lateral membrane in epithelial cells, *Cell 93*, 731−740.
21. Yeaman, C., Grindstaff, K. K., Wright, J. R., and Nelson, W. J. (2001) Sec6/8 complexes on trans-Golgi network and plasma membrane regulate late stages of exocytosis in mammalian cells, *J. Cell. Biol. 155*, 593−604.
22. Inoue, M., Chang, L., Hwang, J., Chiang, S. H., and Saltiel, A. R. (2003) The exocyst complex is required for targeting of Glut4 to the plasma membrane by insulin, *Nature 422*, 629−633.
23. Murthy, M., Garza, D., Scheller, R. H., and Schwarz, T. L. (2003) Mutations in the exocyst component Sec5 disrupt neuronal membrane traffic, but neurotransmitter release persists, *Neuron 37*, 433−447.
24. Murthy, M., and Schwarz, T. L. (2004) The exocyst component Sec5 is required for membrane traffic and polarity in the *Drosophila* ovary, *Development 131*, 377−388.
25. Nicholson, K. L., Munson, M., Miller, R. B., Filip, T. J., Fairman, R., and Hughson, F. M. (1998) Regulation of SNARE complex assembly by an N-terminal domain of the t-SNARE Sso1p, *Nat. Struct. Biol. 5*, 793−802.
26. Munson, M., Chen, X., Cocina, A. E., Schultz, S. M., and Hughson, F. M. (2000) Interactions within the yeast t-SNARE Sso1p that control SNARE complex assembly, *Nat. Struct. Biol. 7*, 894−902.
27. Munson, M., and Hughson, F. M. (2002) Conformational regulation of SNARE assembly and disassembly *in vivo*, *J. Biol. Chem. 277*, 9375−9381.
28. Aalto, M. K., Ronne, H., and Keranen, S. (1993) Yeast syntaxins Sso1p and Sso2p belong to a family of related membrane proteins that function in vesicular transport, *EMBO J. 12*, 4095−4104.
29. Brennwald, P., Kearns, B., Champion, K., Keranen, S., Bankaitis, V., and Novick, P. (1994) Sec9 is a SNAP-25-like component of a yeast SNARE complex that may be the effector of Sec4 function in exocytosis, *Cell 79*, 245−258.
30. Ghaemmaghami, S., Huh, W. K., Bower, K., Howson, R. W., Belle, A., Dephoure, N., O'Shea, E. K., and Weissman, J. S. (2003) Global analysis of protein expression in yeast, *Nature 425*, 737−741.
31. Boyd, C., Hughes, T., Pypaert, M., and Novick, P. (2004) Vesicles carry most exocyst subunits to exocytic sites marked by the remaining two subunits, Sec3p and Exo70p, *J. Cell Biol. 167*, 889−901.
32. Guo, W., Roth, D., Walch-Solimena, C., and Novick, P. (1999) The exocyst is an effector for Sec4p, targeting secretory vesicles to sites of exocytosis, *EMBO J. 18*, 1071−1080.
33. Matern, H. T., Yeaman, C., Nelson, W. J., and Scheller, R. H. (2001) The Sec6/8 complex in mammalian cells: Characterization of mammalian Sec3, subunit interactions, and expression of subunits in polarized cells, *Proc. Natl. Acad. Sci. U.S.A. 98*, 9648−9653.
34. Novick, P., and Guo, W. (2002) Ras family therapy: Rab, Rho, and Ral talk to the exocyst, *Trends Cell Biol. 12*, 247−249.
35. Potenza, M., Bowser, R., Muller, H., and Novick, P. (1992) SEC6 encodes an 85 kDa soluble protein required for exocytosis in yeast, *Yeast 8*, 549−558.
36. Rosen, H. (1957) A modified ninhydrin colorimetric analysis for amino acids, *Arch. Biochem. Biophys. 67*, 10−15.
37. Wiederkehr, A., De Craene, J. O., Ferro-Novick, S., and Novick, P. (2004) Functional specialization within a vesicle tethering complex: Bypass of a subset of exocyst deletion mutants by Sec1p or Sec4p, *J. Cell. Biol. 167*, 875−887.
38. Scholtz, J. M., Barrick, D., York, E. J., Stewart, J. M., and Baldwin, R. L. (1995) Urea unfolding of peptide helices as a model for interpreting protein unfolding, *Proc. Natl. Acad. Sci. U.S.A. 92*, 185−189.
39. Combet, C., Blanchet, C., Geourjon, C., and Deleage, G. (2000) NPS@: Network protein sequence analysis, *Trends Biochem. Sci. 25*, 147−150.
40. Rice, L. M., Brennwald, P., and Brunger, A. T. (1997) Formation of a yeast SNARE complex is accompanied by significant structural changes, *FEBS Lett. 415*, 49−55.
41. Bowser, R., and Novick, P. (1991) Sec15 protein, an essential component of the exocytotic apparatus, is associated with the plasma membrane and with a soluble 19.5S particle, *J. Cell Biol. 112*, 1117−1131.
42. Bowser, R., Muller, H., Govindan, B., and Novick, P. (1992) Sec8p and Sec15p are components of a plasma membrane-associated

19.5S particle that may function downstream of Sec4p to control exocytosis, *J. Cell Biol. 118*, 1041−1056.
43. McBride, H. M., Rybin, V., Murphy, C., Giner, A., Teasdale, R., and Zerial, M. (1999) Oligomeric complexes link Rab5 effectors with NSF and drive membrane fusion via interactions between EEA1 and syntaxin 13, *Cell 98*, 377−386.
44. Price, A., Seals, D., Wickner, W., and Ungermann, C. (2000) The docking stage of yeast vacuole fusion requires the transfer of proteins from a cis-SNARE complex to a Rab/Ypt protein, *J. Cell Biol. 148*, 1231−1238.
45. Sato, T. K., Rehling, P., Peterson, M. R., and Emr, S. D. (2000) Class C Vps protein complex regulates vacuolar SNARE pairing and is required for vesicle docking/fusion, *Mol. Cell 6*, 661−671.
46. Seals, D. F., Eitzen, G., Margolis, N., Wickner, W. T., and Price, A. (2000) A Ypt/Rab effector complex containing the Sec1 homolog Vps33p is required for homotypic vacuole fusion, *Proc. Natl. Acad. Sci. U.S.A. 97*, 9402−9407.
47. Shorter, J., Beard, M. B., Seemann, J., Dirac-Svejstrup, A. B., and Warren, G. (2002) Sequential tethering of Golgins and catalysis of SNAREpin assembly by the vesicle-tethering protein p115, *J. Cell Biol. 157*, 45−62.
48. Suvorova, E. S., Duden, R., and Lupashin, V. V. (2002) The Sec34/Sec35p complex, a Ypt1p effector required for retrograde intra-Golgi trafficking, interacts with Golgi SNAREs and COPI vesicle coat proteins, *J. Cell Biol. 157*, 631−643.
49. Siniossoglou, S., and Pelham, H. R. (2002) Vps51p links the VFT complex to the SNARE Tlg1p, *J. Biol. Chem. 277*, 48318−48324.
50. Conibear, E., Cleck, J. N., and Stevens, T. H. (2003) Vps51p mediates the association of the GARP (Vps52/53/54) complex with the late Golgi t-SNARE Tlg1p, *Mol. Biol. Cell 14*, 1610−1623.
51. Fasshauer, D., Antonin, W., Subramaniam, V., and Jahn, R. (2002) SNARE assembly and disassembly exhibit a pronounced hysteresis, *Nat. Struct. Biol. 9*, 144−151.
52. Barrick, D., and Hughson, F. M. (2002) Irreversible assembly of membrane fusion machines, *Nat. Struct. Biol. 9*, 78−80.
53. Carr, C. M., Grote, E., Munson, M., Hughson, F. M., and Novick, P. J. (1999) Sec1p binds to SNARE complexes and concentrates at sites of secretion, *J. Cell Biol. 146*, 333−344.

BI048008Z